

EhPgp5 mRNA Stability Is a Regulatory Event in the *Entamoeba histolytica* Multidrug Resistance Phenotype*

Received for publication, November 18, 2002, and in revised form, January 27, 2003
Published, JBC Papers in Press, January 28, 2003, DOI 10.1074/jbc.M211757200

César López-Camarillo‡, Juan Pedro Luna-Arias§, Laurence A. Marchat‡, and Esther Orozco¶

From the ‡Programa de Biomedicina Molecular, Escuela Nacional de Medicina y Homeopatía del Instituto Politécnico Nacional and the Departamentos of §Biomedicina Molecular and ¶Patología Experimental, Centro de Investigación y de Estudios Avanzados del Instituto Politécnico Nacional, CP 07300, México, Distrito Federal

The multidrug resistance (MDR) phenotype in *Entamoeba histolytica* is characterized by the overexpression of the *EhPgp5* gene in trophozoites grown in high drug concentrations. Here we evaluated the role of *EhPgp5* mRNA stability on MDR using actinomycin D. *EhPgp5* mRNA from trophozoites growing without emetine had a half-life of 2.1 h, which augmented to 3.1 h in cells cultured with 90 μ M and to 7.8 h with 225 μ M emetine. Polyadenylation sites were detected at 118-, 156-, and 189-nucleotide (nt) positions of the *EhPgp5* mRNA 3'-untranslated region. Interestingly, trophozoites grown with 225 μ M emetine exhibited an extra polyadenylation site at 19 nt. The 3'-untranslated region sequence is AU-rich and has putative consensus sequences for RNA-binding proteins. We detected a RNA-protein complex in a region that contains a polypyrimidine tract (142–159 nt) and a cytoplasmic polyadenylation element (146–154 nt). A longer poly(A) tail in the *EhPgp5* mRNA was seen in trophozoites grown with 225 μ M emetine. Emetine stress may affect factors involved in mRNA turnover, including polyadenylation/deadenylation proteins, which could induce changes in the *EhPgp5* mRNA half-life and poly(A) tail length. Novel evidence on mechanisms participating in *E. histolytica* MDR phenotype is provided.

Entamoeba histolytica, the protozoan parasite responsible for human amoebiasis, presents the multidrug resistance (MDR)¹ phenotype (1) described first in mammalian cells (2) and then in several protozoan parasites (3, 4). MDR is associated with the overexpression of a 170-kDa membrane molecule known as P-glycoprotein (PGP), an energy-dependent pump that extrudes drugs from the cells (5, 6). In *E. histolytica*, MDR phenotype is given mainly by overexpression of the *EhPgp1* and *EhPgp5* genes, which are finely regulated by transcriptional factors (7–9). Although *EhPgp1* is constitutively expressed in drug-resistant trophozoites of clone C2, *EhPgp5*

gene is overexpressed only when C2 cells are grown in a high emetine concentration (10, 11). Both genes are also amplified in the presence of a high drug concentration (12).

Transcriptional regulation of eukaryotic *mdr* genes has been considered as the major control point for PGP synthesis, although gene amplification mechanisms also participate in this event (12, 13). Moreover, there is growing evidence of pivotal post-transcriptional (14–17) and post-translational (18–20) regulation of the PGP expression. On the other hand, mRNA stability has recently emerged as a critical control step in determining cellular stationary mRNA levels. The abundance of a particular mRNA can fluctuate many folds due to alterations in mRNA stability without any change in the transcription rate (21). The mRNA half-life is determined by a complex set of protein interactions at the 3'-untranslated region (3'-UTR) depending on conserved cis-element sequences and secondary structures (for review, see Ref. 22). The 3'-UTR also contains consensus sequence elements that mediate mRNA nuclear export, cytoplasmic localization, translation efficacy, and polyadenylation control (23, 24). The pre-mRNAs are polyadenylated in a reaction involving 3' endonucleolytic cleavage followed by poly(A) tail synthesis (25). Poly(A) tail is also a modulator of mRNA stability and translation (26, 27). Strict control of poly(A) tail length is achieved by the concerted interplay of key factors, including poly(A) polymerase, deadenylases, and poly(A)-binding protein activities (25).

Several reports have addressed the importance of mRNA stability on the *mdr* genes expression regulation. *Pgp1*, *Pgp2*, and *Pgp3* mRNAs have a higher half-life in rat tumor cells than in normal cells (15), whereas rat MDR hepatocytes in culture present a higher amount of PGP2 protein due to a post-transcriptional mechanism controlling mRNA stability (14). Human *MDR1* mRNA has a half-life of 30 min, which is prolonged to more than 20 h upon treatment with cycloheximide, suggesting that protein synthesis inhibition may influence the stability of certain mRNAs (16, 17). However, molecular mechanisms controlling *mdr* mRNA stability remains to be elucidated.

In *E. histolytica*, mRNA stability mechanisms have not been studied yet. The presence of higher levels of EhPGP5 protein in the multidrug-resistant trophozoites of clone C2 could be influenced by both transcriptional activation and increased mRNA stability. In this paper, we measured the *EhPgp5* mRNA half-life in trophozoites of clone C2 grown at different emetine concentrations. Our data showed that *EhPgp5* mRNA stability is increased at high emetine concentrations, indicating that mRNA half-life is also regulating the MDR phenotype. In addition, here we initiated the study of the mechanisms involved in mRNA turnover in this parasite.

* This work was supported by a grant from the Howard Hughes Medical Institute (to E. O.) and by Consejo Nacional de Ciencia y Tecnología (México) and European Community grants. The costs of publication of this article were defrayed in part by the payment of page charges. This article must therefore be hereby marked "advertisement" in accordance with 18 U.S.C. Section 1734 solely to indicate this fact.

¶ To whom correspondence should be addressed. Tel.: 52-55-5747-3800 (ext. 5650); Fax: 52-55-5747-7108; E-mail: esther@mail.cinvestav.mx.

¹ The abbreviations used are: MDR, multidrug resistance; PGP, P-glycoprotein; Py, polypyrimidine tracts; CPE, cytoplasmic polyadenylation element; UTR, untranslated region; RT, reverse transcriptase; MOPS, 4-morpholinepropanesulfonic acid; CE, cytoplasmic extracts; LM-PAT, ligase-mediated poly(A) test; nt, nucleotide(s); PS, polyadenylation signals; AURE, AU-rich element.

EXPERIMENTAL PROCEDURES

E. histolytica Cultures—Trophozoites of the clones A (drug-sensitive) and C2 (drug-resistant) (strain HM1:IMSS) (28) were axenically cultured in TYI-S-33 medium (29). Trophozoites of clone C2 were cultured without emetine (C2) or with 90 (C2(90)) and 225 (C2(225)) μM emetine. Logarithmic phase growing cultures were used in all experiments. All assays presented here were performed at least three times by duplicate.

Transcriptional Inhibition by Actinomycin D—Actinomycin D (Roche Molecular Biochemicals) dissolved in dimethyl sulfoxide (Me_2SO) (0.5 mg/ml) was added to the trophozoites cultures to a final concentration of 10 $\mu\text{g}/\text{ml}$ of medium, and cells were incubated at 37 °C for different times. Fresh medium supplemented with [^3H]UTP (10 $\mu\text{Ci}/\text{ml}$) was added to the actinomycin D-treated trophozoites for 2 more hours in the absence of actinomycin D. Immediately, total RNA was isolated by TRIzol[®] (Invitrogen). Incorporation of [^3H]UTP in 20 μg of total RNA was measured by liquid scintillation counting system (Beckman) in duplicate samples, and data obtained were plotted. Cytotoxicity of actinomycin D and Me_2SO was checked by cell viability using trypan blue and measuring the growth rate of the treated cultures.

Reverse Transcriptase (RT)-PCR Experiments—100 ng of total RNA from trophozoites of clones A, C2, C2(90), and C2(225) were preincubated at 37 °C for 15 min with 10 units of RNase-free DNase I (Stratagene). Single-stranded cDNAs were synthesized using 10 mM each dNTP and 100 ng of oligo(dT)₁₈ in diethyl pyrocarbonate-treated water. The mixture was heat-denatured at 65 °C for 5 min and quick-chilled on ice. Then we added buffer used to synthesize the first-strand (50 mM Tris-HCl, pH 8.3, 75 mM KCl, 3 mM MgCl_2), 100 mM dithiothreitol, 200 units of Superscript[™] II RNase H⁻ reverse transcriptase (Invitrogen), and 40 units of SUPERase-in ribonuclease inhibitor (Ambion). This mixture was incubated at 42 °C for 1 h. To remove the excess RNA template, 2 units of RNase H (Amersham Biosciences) were added, and the mixture was incubated at 37 °C for 15 min. Quantitative multiplex PCR for *EhPgp5* and actin cDNAs were performed with 1/5 volume of the reverse transcription mixture, 10 mM each dNTPs, 5 mM MgCl_2 , 2.5 units of *Taq* DNA polymerase (Invitrogen), and the *EhPgp5* (5'-GTAG-GAGGTGCGATATTTC-3') sense and (5'-CCATCCTATTCCTGTTT-GAC-3') antisense internal primers (30). The actin (5'-AGCTGTTCTT-TCATTATATGC-3') sense and (5'-TTCTCTTTCAGCAGTAGTGGT-3') antisense internal primers (31) were used in the same sample as an internal control. PCR was done in 22 cycles at 95 °C for 30 s, 52 °C for 35 s, 72 °C for 90 s, and a final extension step at 72 °C for 7 min. Amplified products were separated by 6% PAGE.

EhPgp5 mRNA Stability Assays—Total RNA from trophozoites of clones C2, C2(90), and C2(225) was obtained at 0, 2, 4, 8, and 12 h after actinomycin D-induced transcriptional blockage. *EhPgp5* and actin mRNAs were measured by multiplex RT-PCR as described above, and intensity of the bands in ethidium bromide-stained gels was quantified by densitometric analysis in a PhosphorImager apparatus (Personal Molecular Imager FX, Bio-Rad). The pixels given by the actin transcript in trophozoites of clones C2, C2(90), and C2(225) without treatment (t_0) were taken as 100% in each clone. *EhPgp5* mRNA levels were normalized with respect to the actin amount in each lane. Experimental *EhPgp5* mRNA half-life (the time at which 50% of mRNA molecules remained intact) was determined by plotting the *EhPgp5* mRNA amount at different times on a semilogarithmic scale. In these estimations the *EhPgp5* mRNA amount at t_0 was taken as 100% in each clone. Theoretical half-life of the *EhPgp5* mRNA was obtained from the logarithmically transformed best-fit line by linear regression analysis using the decay equation $t_{1/2} = \ln 2/K$, where K corresponds to the decay constant (32).

S1 Nuclease Mapping Experiments—20 μg of total RNA from trophozoites of clones C2, C2(90), and C2(225) were hybridized with a 697 bp of [α - ^{32}P]dATP (PerkinElmer Life Sciences)-labeled probe corresponding to the last 100 bp of the *EhPgp5* coding region and 597 bp of the *EhPgp5* 3'-UTR genomic sequence. The probe was PCR-amplified from the P4 plasmid, which contains the last 1466 bp of the *EhPgp5*-coding region and ~1500 bp of its 3'-UTR genomic sequence (7), using the *EhPgp5*-3'-UTR-S (5'-AAAATAGTAGAACAAGGA-3') sense and *EhPgp5*-3'-UTR-AS (5'-CGAACAAAGGCTTAAA-3') antisense primers. Amplified *EhPgp5*-3'-UTR fragment was sequenced in an ABI PRISM automatic sequencer. Purified DNA probe was heat-denatured at 95 °C for 15 min and cooled at 4 °C for 3 min. Then, an RNA aliquot was added, and immediately, the DNA/RNA hybrid mixture was co-precipitated with ethanol at -20 °C overnight. A DNA/RNA pellet was collected by centrifugation, air-dried, and resuspended in 20 μl of S1 nuclease hybridization buffer (80% deionized formamide, 40 mM MOPS, pH 7, 400 mM NaCl, and 1 mM EDTA). The DNA/RNA hybrids were

fully denatured at 85 °C for 10 min and subsequently incubated at 42 °C overnight. Then, samples were 10-fold diluted and treated with 1250 units of S1 nuclease (Invitrogen) at 37 °C for 1 h in the reaction buffer (300 mM sodium acetate, pH 4.6, 1 mM NaCl, and 10 mM zinc acetate). At the same time, we performed a sequencing reaction of the *EhPgp5* 3'-UTR using the *EhPgp5*-3'-UTR-S primer. The sequencing products and RNA fragments protected of the S1 nuclease digestion were resolved through denaturing 8% PAGE at room temperature, vacuum-dried, and visualized in a PhosphorImager apparatus.

In Vitro Transcription—Templates for transcript synthesis were prepared from pBluescript II SK (+/-) phagemid (pBS) (Stratagene), which contains the T7 λ phage promoter. The PSI¹⁹, PSII¹¹⁸, PSIII¹⁵⁶, and PSIV¹⁸⁹ DNA fragments that contain the last 100 bp of *EhPgp5* open reading frame and 19, 118, 156, and 189 bp of the 3'-UTR, respectively, were PCR-amplified using 1 unit of Deep Vent DNA polymerase (New England Biolabs) and the P4 plasmid (7) as template. The primers used were *EhPgp5*-3'-UTR-S sense and the PSI-AS (5'-TTAATATTTATATGAATTA-3'), PSII-AS (5'-TTATTATGAATGATA-AATA-3'), PSIII-AS (5'-AAAGAATAAAAACAAACT-3'), and PSIV-AS (5'-TATCATATAACAATTA-3') antisense primers. Amplified products were directionally cloned into the *Bam*HI and *Xho*I sites of pBS plasmid and sequenced in an ABI PRISM automatic sequencer. Recombinant plasmids (1 μg each) were linearized with *Xho*I restriction enzyme and *in vitro* transcribed with T7 RNA polymerase using 1 mM each NTP, 100 mM dithiothreitol, and 40 units of recombinant RNasin ribonuclease inhibitor (Invitrogen) at 37 °C for 1 h according to the manufacturer protocol (Promega). Labeled *EhPgp5* 3'-UTR RNA fragments were produced by the addition of [α - ^{32}P]UTP (3000 Ci/mmol) (PerkinElmer Life Sciences) in the synthesis reaction. Finally, RNase-free DNase (10 units) was added, and the mixture was incubated at 37 °C for 15 min to remove DNA templates. Labeled RNA probes were purified by Sephadex G50 column filtration. *EhPgp5* 3'-UTR transcripts length was determined by 12% denaturing PAGE.

Cytoplasmic Extracts—Cytoplasmic extracts (CE) were obtained as described (33) with some modifications for *E. histolytica*. Briefly, 1×10^6 trophozoites of clones C2, C2(90), and C2(225) were washed with 1 ml of phosphate-buffered saline, pH 6.8, supplemented with 10 mM HEPES, pH 7.9, 1.5 mM MgCl_2 , 10 mM KCl, 0.5 mM dithiothreitol, and 0.5 mM phenylmethylsulfonyl fluoride and incubated on ice for 15 min. Then 25 μl of 10% Nonidet P-40 and protease inhibitor mixture (0.5 mM phenylmethylsulfonyl fluoride, 2 mM benzamide, 5 $\mu\text{g}/\text{ml}$ each aprotinin, pepstatin A, leupeptin, and E-64) were added, and samples were vortexed for 10 s and centrifuged at 12,000 $\times g$ at 4 °C for 1 min. The supernatant was mixed with 0.11 volume of 100 mM HEPES, pH 7.9, 30 mM MgCl_2 , 250 mM KCl solution and centrifuged at 14,000 $\times g$ at 4 °C for 1 h. Protein concentration was determined by the Bradford method (34).

RNA Electrophoretic Mobility Shift Assays— 5×10^5 cpm of each PSI¹⁹, PSII¹¹⁸, PSIII¹⁵⁶, and PSIV¹⁸⁹ [α - ^{32}P]UTP-labeled probes and 60 μg of CE were separately incubated in the binding buffer (10 mM HEPES, pH 7.9, 40 mM KCl, 1 mM dithiothreitol, 4 mM MgCl_2 , 4 mM spermidine, 5% glycerol) at 4 °C for 15 min in 20 μl of final volume. Subsequently, RNase A + T₁ (10 μg + 20 units) (Sigma) were added to the mixture and incubated at room temperature for 15 min. Then, heparin (5 mg/ml) was added, and the mixture was incubated for an additional 10 min. For competition assays, we used a 350-fold molar excess of the PSI¹⁹-, PSII¹¹⁸-, PSIII¹⁵⁶-, and PSIV¹⁸⁹-unlabeled probes. RNA-protein complexes were resolved at 130 V for 4 h on pre-electrophoresed 6% nondenaturing PAGE. Gels were vacuum-dried, and RNA-protein interactions were detected by scanning in a PhosphorImager apparatus.

Analysis of Poly(A) Tail Length—Total RNA was used for ligase-mediated poly(A) test (LM-PAT) according to the method described (35). 1 μg of total RNA was incubated at 37 °C for 15 min with 10 units of RNase-free DNase I (Stratagene). Annealing and *in situ* ligation of 20 ng of oligo(dT)₁₈ to the 3' end of poly(A) tails of total RNA were done at 42 °C for 30 min in diethyl pyrocarbonate-treated water. Subsequent annealing of 200 ng of hybrid oligo(dT)₁₈-adapter primer (5'-GACTC-GAGTCGACATCGAT₁₈-3') was done at 12 °C for 2 h. cDNA synthesis was performed using the first-strand buffer, 100 mM dithiothreitol, 200 units of Superscript[™] II, and recombinant RNasin ribonuclease inhibitor (40 units) at 42 °C for 1 h. PCR was performed using 1/10 volume of the samples and the (5'-CTGAGCTCAGCTGTAGCT-3') antisense primer complementary to the adapter region of the oligo(dT)₁₈-adapter primer and the *EhPgp5*-3'-UTR-S sense oligonucleotide. An actin 3'-UTR (5'-GATCAATTCTTGCCCTCAT-3') sense primer was used as a control. Amplification for *Ehgp5* and actin genes was done in 30 cycles at 95 °C at 30 s, 59 °C at 35 s, 72 °C at 90 s, and a final extension step

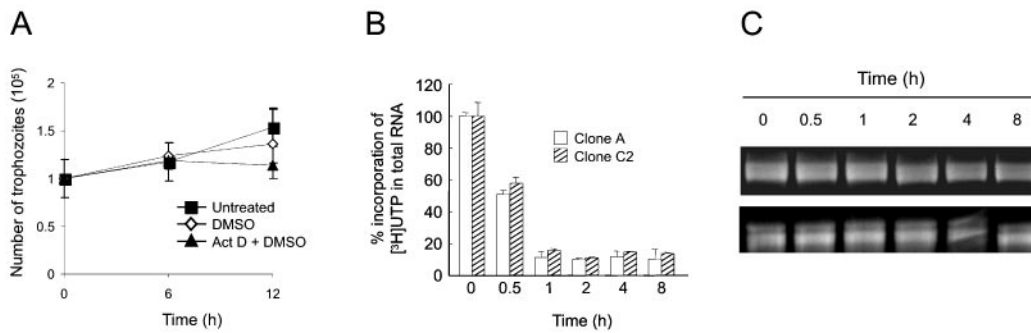


FIG. 1. **Effect of actinomycin D on RNA synthesis in the *E. histolytica* trophozoites of clones A and C2.** A, growth curve of the trophozoites of clone C2 treated with actinomycin D. B, effect of actinomycin D on RNA synthesis in the trophozoites of clones A and C2. Actinomycin D-treated trophozoites were incubated with [³H]UTP (10 μCi/mmol) for 2 h, and incorporation was measured in 20 μg of total RNA. Incorporation values at *t*₀ were taken as 100% for each clone. Bars represent the average of three duplicate experiments. C, formaldehyde-agarose gel (1.2%) showing the recombinant RNA obtained from actinomycin D-treated trophozoites of clones A (upper panel) and C2 (lower panel) at the indicated times. DMSO, dimethyl sulfoxide.

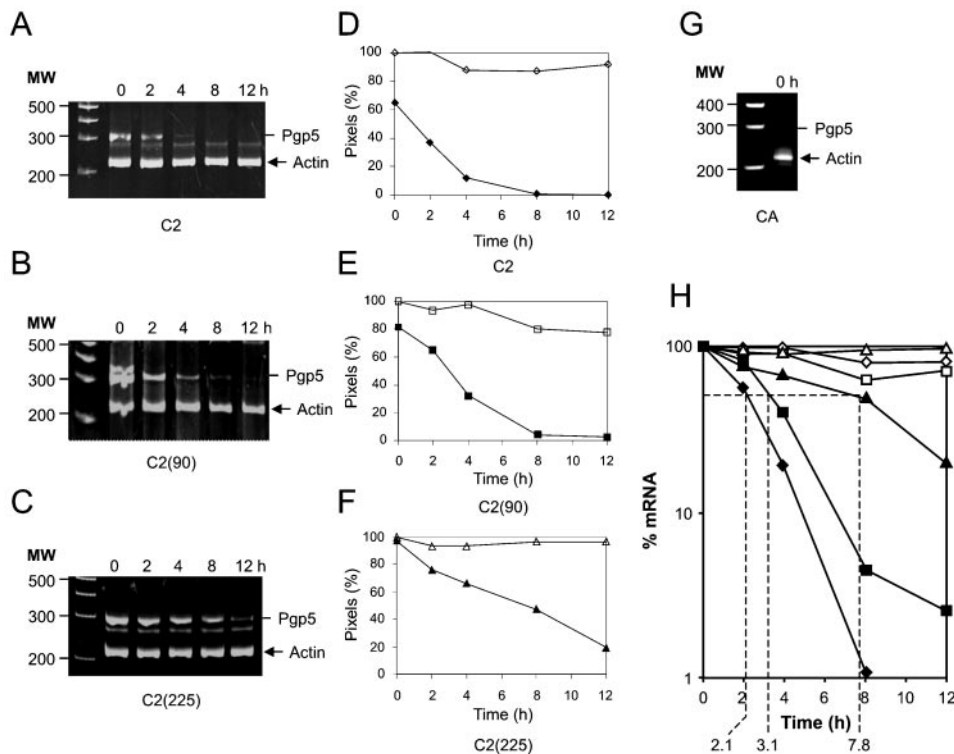


FIG. 2. **Determination of the *EhPgp5* mRNA half-life.** A–C and G, ethidium bromide-stained gels showing the RT-PCR products obtained at different times after actinomycin D transcriptional blockage. MW, molecular weight. D–F, densitometric analysis of RT-PCR products in A–C. H, semilogarithmic plot of the *EhPgp5* and actin mRNA levels quantified by densitometry in A–C. The graphics showed the results of a representative assay of three independent experiments. Actin: ◇, C2; □, C2(90); △, C2(225). *EhPgp5*: ◆, C2; ■, C2(90); ▲, C2(225).

at 72 °C for 7 min. PCR samples were separated on a 1.5% Tris-buffered EDTA-agarose gel then transferred to nylon membranes and hybridized with specific *EhPgp5* and actin 3'-UTR [^α-³²P]dATP-labeled probes.

RESULTS

Actinomycin D Inhibits E. histolytica Transcription—To study the mechanisms controlling mRNA decay in *E. histolytica* we first investigated the effect of the transcription inhibitor actinomycin D on viability, growth, and mRNA synthesis in trophozoites of the drug-sensitive clone A and drug-resistant clone C2. Cell viability of trophozoites of clone C2 incubated 12 h with or without actinomycin D was 98%. At this time cell growth was slightly delayed in the actinomycin D-treated trophozoites in comparison with untreated cells (Fig. 1A). The effect of actinomycin D on cell growth and viability was similar in trophozoites of all clones tested (data not shown). Then we performed experiments to determine whether mRNA synthesis

was affected by actinomycin D and the time required to inhibit at least 90% of mRNA synthesis. Results showed that actinomycin D affects the [³H]UTP incorporation into new synthesized RNA in a time-dependent manner (Fig. 1B). Untreated trophozoites of clones A and C2 incubated for 2 h (*t*₀) with [³H]UTP incorporated 16,450 and 14,660 cpm, respectively. Each value was taken as 100% incorporation for the corresponding clone (Fig. 1B). Trophozoites of clones A and C2 preincubated for 30 min with the drug and then incubated with [³H]UTP for 2 h incorporated 50.4 and 59.9% of radioactivity, respectively. One hour later, both clones presented only 12% incorporation of [³H]UTP (Fig. 1B). These low levels of RNA synthesis were maintained in trophozoites of both clones incubated with actinomycin D for up to 8 h (Fig. 1B). As a control for mRNA integrity, equivalent amounts of total RNA were isolated at each time, and rRNA were visualized in ethidium

TABLE I

Theoretical and experimental *EhPgp5* mRNA half-life in *E. histolytica* trophozoites of clone C2 grown at different emetine concentrations ND, Not determined.

	Theoretical mRNA half-life ^a		Experimental mRNA half-life ^b	
	<i>EhPgp5</i>	Actin	<i>EhPgp5</i>	Actin
	(h)		(h)	
C2	1.2	ND	2.1	>12
C2 (90)	2.7	ND	3.1	>12
C2 (225)	5.6	ND	7.8	>12
CA	ND	ND	ND	ND

^a According to the decay equation: $t_{1/2} = \ln 2/K$.

^b According to the semilogarithmic data plotted in Fig. 2H.

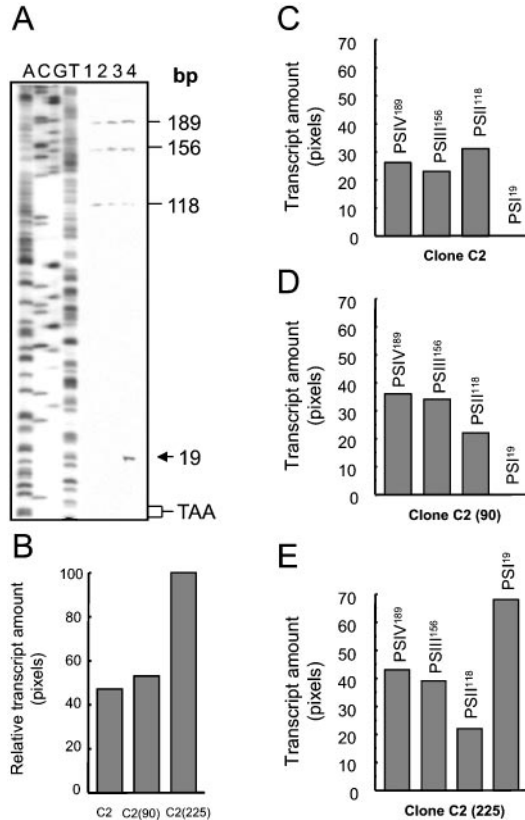


FIG. 3. Determination of the *EhPgp5* mRNA polyadenylation sites. 20 μ g of total RNA from trophozoites of clones C2, C2(90), and C2(225) were hybridized with a genomic *EhPgp5* 3'-UTR probe and then digested with S1 nuclease. A, 8% PAGE analyzed products alongside *EhPgp5* 3'-UTR sequence ladder. Numbers at the right indicate the size of protected fragments. Lane 1, tRNA negative control hybridization; lane 2, clone C2; lane 3, clone C2(90); lane 4, clone C2(225). The arrow shows the extra polyadenylation site detected in trophozoites of clone C2(225). TAA indicates the translation stop codon position. B, representative data of the analysis by densitometry of bands in A. Total pixels obtained from the transcript species in clone C2(225) were taken as 100%, and those from C2(90) and C2 clones were expressed in relation to it. C-E, graphic representations of the relative amounts of each transcript variant in all clones. These assays were performed three times, and relative transcript values were reproducible.

bromide-stained agarose gels (Fig. 1C). No appreciable changes in the rRNA amount were observed, indicating no significant RNA degradation. These data provided us a temporal window in which the mRNA decay could be analyzed.

EhPgp5 mRNA Stability Is Higher in Trophozoites of the Clone C2 Cultured with Emetine—To investigate the *EhPgp5* mRNA stability in trophozoites growing with different emetine concentrations, we determined the *EhPgp5* mRNA half-life in actinomycin D-treated trophozoites of clones C2, C2(90), and

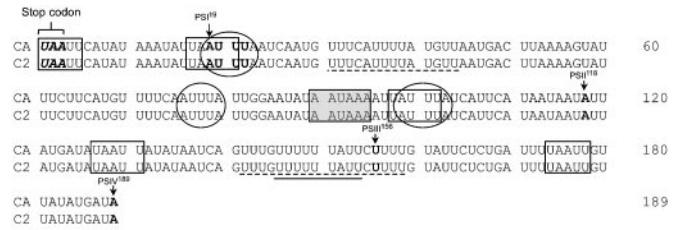


FIG. 4. Sequence of the 189 bp *EhPgp5* 3'-UTR of clones A and C2. Arrows show the position of the four polyadenylation sites mapped (PSI¹⁹, PSII¹¹⁸, PSIII¹⁵⁶, and PSIV¹⁸⁹). *E. histolytica* consensus polyadenylation signals (UA(A/U)UU) are in open boxes. Eukaryotic poly(A) signal (AAUAAA) is indicated by a shadowbox. Continuous and discontinuous underlines denote the CPE motif and the polypyrimidines tract, respectively. Ellipses denote the AU-rich elements (AUUUA). Numbers at the right are relative to the translation stop codon (position 1).

C2(225). *EhPgp5* mRNA was measured from 0 to 12 h by semiquantitative RT-PCR assays in total RNA. We included actin primers in all reactions as internal control. Results showed that *EhPgp5* mRNA was present in untreated trophozoites of clone C2, and the signal diminished progressively at 2 and 4 h after the transcriptional blockage (Fig. 2A). In clone C2(90), the *EhPgp5* transcript was detected up to 8 h after actinomycin D treatment (Fig. 2B). Interestingly, in clone C2(225) the *EhPgp5* mRNA was detected even 12 h after the transcriptional blockage (Fig. 2C). These data indicated that *EhPgp5* mRNA amounts are reduced in a time-dependent manner in actinomycin D-treated trophozoites, but they are maintained for a longer time in the emetine-cultured cells. In contrast, we did not detect the *EhPgp5* mRNA in untreated trophozoites of the wild type drug-sensitive clone A (Fig. 2G), confirming that *EhPgp5* gene is not transcribed in the drug-sensitive trophozoites (36).

The *EhPgp5* and actin mRNAs were quantified by densitometry and arbitrary expressed in pixels (Fig. 2, D-F). Pixels given by actin at t_0 were taken as 100% in each clone, and the *EhPgp5* percentage was expressed with respect to the actin mRNA levels. At t_0 , the actin amount appeared almost unaltered, whereas *EhPgp5* varied in the three clones. In trophozoites of clone C2, the *EhPgp5* mRNA was 63% of the actin mRNA (Fig. 2D), and in C2(90) it was 81% (Fig. 2E), whereas clone C2(225) exhibited similar levels of both transcripts (Fig. 2F). The other bands seen in the gels were not related to the *EhPgp5* transcript, as probed by Southern blot hybridization using the *EhPgp5* probe (data not shown).

To determine the experimental mRNA half-life, the results of normalized *EhPgp5* mRNA levels were plotted in a semilogarithmic scale against the exposure time to actinomycin D (Fig. 2H). In these calculations, the amount of *EhPgp5* and actin mRNA at t_0 was taken as 100% in each clone. In trophozoites of clone C2, the experimental *EhPgp5* mRNA half-life was estimated in 2.1 h, whereas in C2(90) it was 3.1 h and 7.8 h in C2(225), confirming significant variations in the decay rates of the three clones. In addition, these experiments showed that actin mRNA decay remained with minimal changes during the 12-h course of the transcription inhibition in all clones. There are reports proposing that actin mRNA has a half-life between 24 and 33 h in mammalian cells (37). According to our experiments, *E. histolytica* actin mRNA has a half-life longer than 12 h.

Experimental values were close to the theoretical *EhPgp5* mRNA half-life predicted from the decay equation described under "Experimental Procedures." The theoretical *EhPgp5* mRNA half-life was 1.2 h in the trophozoites of clone C2, 2.7 h in C2(90), and increased to 5.6 h in C2(225) (Table I).

EhPgp5 mRNA Presents 3'-UTR Heterogeneity—To determine whether the distinct *EhPgp5* mRNA half-lives observed

A

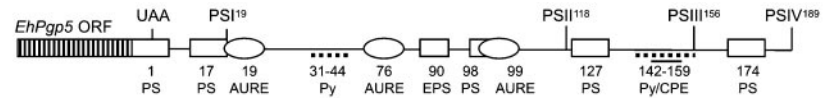
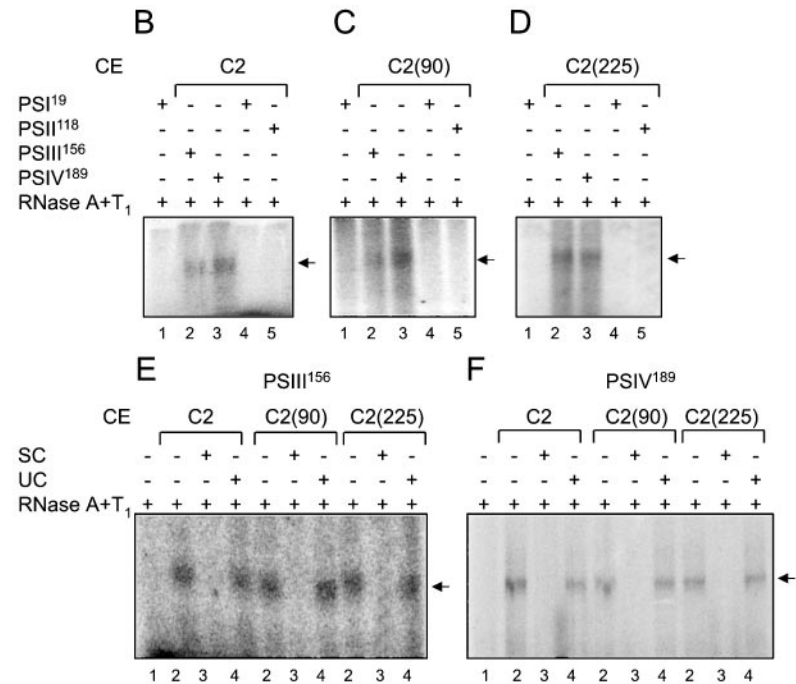


FIG. 5. RNA-protein complex formation in the *EhPgp5* 3'-UTR mRNA. **A**, schematic representation of the putative cis-acting elements present in the 3'-UTR of the *EhPgp5* fragments used for RNA electrophoretic mobility shift assays. *EPS*, eukaryotic polyadenylation signal; *UAA*, stop codon. *ORF*, open reading frame. **B–D**, [α - 32 P]UTP-labeled *PSI*¹⁹, *PSII*¹¹⁸, *PSIII*¹⁵⁶, and *PSIV*¹⁸⁹ probes were incubated with CE from trophozoites of the different clones, as described under "Experimental Procedures." *Lane 1*, free *PSI*¹⁹; *lane 2*, *PSIII*¹⁵⁶; *lane 3*, *PSIV*¹⁸⁹; *lane 4*, *PSI*¹⁹; and *lane 5*, *PSII*¹¹⁸ probes. **E** and **F**, competition experiments. The *PSIII*¹⁵⁶ (**E**) and *PSIV*¹⁸⁹ (**F**) riboprobes were incubated with CE from the trophozoites in the presence of free probe (*lane 1*), no competitor (*lane 2*), specific competitor (*SC*; *lane 3*) (350-fold molar excess of homologous unlabeled fragments), and unspecific competitor (*UC*; *lane 4*) (350-fold molar excess of tRNA). Arrows denote RNA-protein complex.



in the trophozoites of clones C2, C2(90), and C2(225) could be influenced by changes in the 3'-UTR length, we performed RNA protection assays with S1 nuclease (Fig. 3A). Three RNA-DNA-protected fragments were found at nt 118, 156, and 189 downstream of the UAA stop codon of the *EhPgp5* mRNA in all C2 clones (Fig. 3A, lanes 2–4). These fragments, corresponding to different *EhPgp5* 3'-UTR variants, were denoted as *PSII*¹¹⁸, *PSIII*¹⁵⁶, and *PSIV*¹⁸⁹, respectively. Interestingly, clone C2(225) showed an extra protected fragment at the nt 19 (*PSI*¹⁹) (Fig. 3A, arrow). The protected fragments detected were analyzed by densitometry (Fig. 3B). The total pixels obtained from the transcript species in clone C2(225) were taken as 100%, and those from C2(90) and C2 clones were 53 and 47%, respectively. In clone C2, the *PSIV*¹⁸⁹, *PSIII*¹⁵⁶, and *PSII*¹¹⁸ variants showed levels of 26, 23, and 31 pixels, respectively (Fig. 3C). In clone C2(90), *PSIV*¹⁸⁹ and *PSIII*¹⁵⁶ appeared in similar amounts (36 and 34 pixels), whereas *PSII*¹¹⁸ gave only 21 pixels (Fig. 3D). In clone C2(225), the transcript *PSI*¹⁹ was 40% of total variants (68 pixels), whereas *PSIV*¹⁸⁹, *PSIII*¹⁵⁶, and *PSII*¹¹⁸ gave 43, 39, and 23 pixels, respectively (Fig. 3E). In clone C2(225), the *PSIII*¹⁵⁶ and *PSIV*¹⁸⁹ species increased almost 2-fold with respect to *PSII*¹¹⁸, whereas *PSI*¹⁹ was 3.3-fold, suggesting that they could be more stable (Fig. 3E).

The presence of various polyadenylation sites suggested that mRNA variants could influence the *EhPgp5* mRNA steady-state levels, as has been reported for other cells (38–40). Differences in sequence at the 3'-UTR could be involved in the *EhPgp5* mRNA stability and polyadenylation site selection. The comparative analysis of the first 189 bases in the 3'-UTR *EhPgp5* DNA showed that 3'-UTR sequences were identical in clones A, C2 (Fig. 4), and C2(225) clones (data not shown), indicating that differences in sequence do not account for the *EhPgp5* mRNA half-life or for the polyadenylation site choice.

The *EhPgp5* 3'-UTR is 85% AU-rich, and it presents several putative consensus binding sequences for regulatory proteins. There are five putative consensus polyadenylation signals (PS) with the UA(A/U)UU sequence described for *E. histolytica* (41) at nt 1, 17, 98, 127, and 174 (Fig. 4, open boxes). We also found several eukaryotic 3'-UTR elements including the canonical polyadenylation signal (AAUAAA) at nt 90 (Fig. 4, shadowbox) and three putative AU-rich elements (AUREs) conformed by the conserved AUUUA sequence (42) at nt 19, 76, and 99 downstream from the UAA codon (Fig. 4, ellipses). In addition, two polypyrimidine tracts (Py) were detected at nt 31–44 and 142–159 (Fig. 4, discontinuous underlined) and a consensus cytoplasmic polyadenylation element (CPE), (UUUUUAU) at nt 146–154 (Fig. 4, continuous underlined). The CPE seems to promote cytoplasmic polyadenylation in eukaryotic cells (43). Alignment of the *EhPgp5* 3'-UTR full-length with other *mdr* 3'-UTR sequences revealed a high divergence between 3'-UTRs *mdr* gene family members (data not shown).

A Specific RNA-Protein Complex Was Detected at the *EhPgp5* 3'-UTR mRNA—Stability of mRNA is also regulated through site-specific binding of cytoplasmic proteins to consensus sequences at the 3'-UTR mRNA. The presence of putative *EhPgp5* mRNA binding regulatory proteins was investigated by RNA electrophoretic mobility shift assays using the *PSI*¹⁹, *PSII*¹¹⁸, *PSIII*¹⁵⁶, and *PSIV*¹⁸⁹ fragments as RNA probes (Fig. 5A). The results showed that *PSIII*¹⁵⁶ and *PSIV*¹⁸⁹ transcripts were able to form a RNA-protein complex with CE from C2, C2(90), and C2(225) clones (Fig. 5, B–D, lanes 2 and 3). RNA-protein complex was specifically competed by a 350-fold molar excess of the same unlabeled transcript, but they were maintained in the presence of tRNA, used as nonspecific competitor (Fig. 5, E and F, lanes 3 and 4). The intensity and migration of the RNA-protein complex was similar in all clones (Fig. 5, B–F).

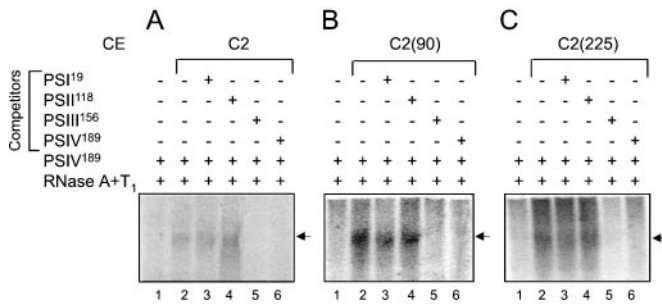


FIG. 6. Competition of the RNA-protein complex formed in the PSIV¹⁸⁹ *EhPgp5* transcript. [α -³²P]UTP-labeled full-length PSIV¹⁸⁹ probe was incubated with CE (lanes 2–6) from trophozoites of the different clones in the presence of different unlabeled probe competitors. Lane 1, free probe; lane 2, no competitor; lane 3, PSI¹⁹; lane 4, PSII¹¹⁸; lane 5, PSIII¹⁵⁶; lane 6, PSIV¹⁸⁹ probes. Arrows show the RNA-protein complex.

In contrast, we did not find any RNA-protein complex when we used PSI¹⁹ and PSII¹¹⁸ fragments (Fig. 5, B–D, lanes 4 and 5).

To delimitate the region in which the RNA-protein complex was formed, we carried out cross-competition experiments using the PSIV¹⁸⁹ transcript as labeled probe and the PSI¹⁹, PSII¹¹⁸, and PSIII¹⁵⁶ RNAs as competitors. In the three clones the complex formed in the PSIV¹⁸⁹ region was specifically competed by the same probe and by PSIII¹⁵⁶ (Fig. 6, A–C, lanes 5 and 6) but not by PSI¹⁹ and PSII¹¹⁸ RNA fragments, as expected (Fig. 6, A–C, lanes 3 and 4). These results suggest that RNA-protein interaction takes place in a region of 38 nt (nt 119–156), which is shared by PSIII¹⁵⁶ and PSIV¹⁸⁹ fragments. This region contains a PS (nt 127–131) and a 15-nt Py (nt 142–156) sequences, including a CPE (nt 146–154) motif, which could be targets for regulatory RNA-binding proteins (43–46).

The EhPgp5 mRNA Poly(A) Tail Is Longer in C2(225) Trophozoites—Poly(A) tail is an important modulator of mRNA turnover, and its length is subjected to cellular control throughout the life span of the mRNA (25). We investigated the poly(A) tail length of *EhPgp5* mRNA from trophozoites of clones C2, C2(90), and C2(225) by LM-PAT (35), as described under “Experimental Procedures.” We observed three well defined bands corresponding to the PSII¹¹⁸, PSIII¹⁵⁶, and PSIV¹⁸⁹ predicted transcripts plus 100 bp of the *EhPgp5* open reading frame, respectively (Fig. 7A). In these assays, we could not amplify the PSI¹⁹ variant, probably because *EhPgp5* PSI¹⁹ transcript has a very short poly(A) tail. The identity of the amplified products was confirmed by Southern blot hybridization with a DNA probe containing the last 100 bp of the open reading frame and the first 19 nt of the *EhPgp5* mRNA 3'-UTR (Fig. 7B). The signal appeared as a smear ranging from 218 to 300 nt in mRNA from trophozoites of clones C2 and C2(90) (Fig. 7B). Interestingly, in clone C2(225) the hybridization signal showed a longer smear spanning from 218 to 500 nt. The same membrane hybridized with the actin 3'-UTR probe gave no signal (Fig. 7C). In contrast, in the actin control assays, we detected a defined 130-bp band corresponding to actin 3'-UTR (~30 nt) plus 99 bases of the 3'-actin open reading frame and a short smear spanning 130–150 nt in all clones (Fig. 7, D and E). The actin control membrane gave no signal with the *EhPgp5* 3'-UTR probe (Fig. 7F).

These LM-PAT patterns represent an enlargement of the poly(A) tail length of the *EhPgp5* mRNA in the trophozoites of clone C2(225) or, alternatively, a shortening in C2 and C2(90) cells, suggesting that changes in poly(A) tail length are involved in *EhPgp5* mRNA half-life.

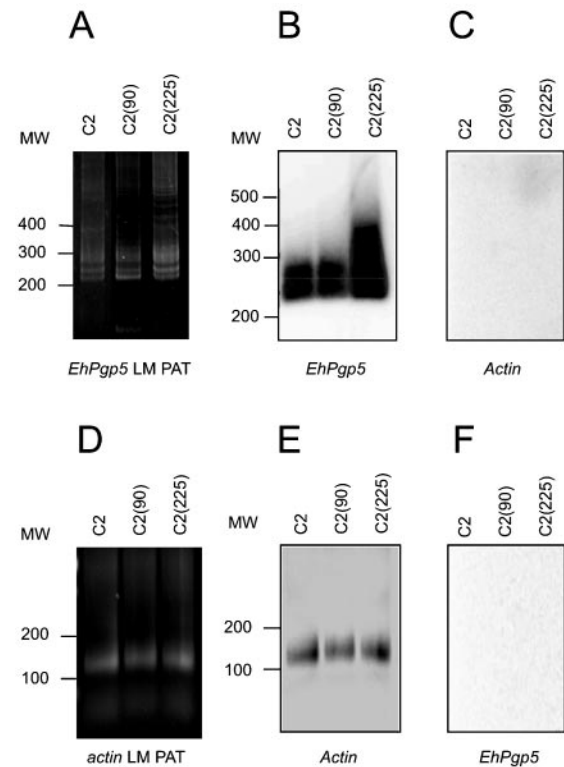


FIG. 7. LM-PAT of *EhPgp5* and actin mRNAs. Ethidium bromide-stained agarose gels (1.5%) of the *EhPgp5* (A) and actin (D) LM-PAT-amplified products using RNA from trophozoites of the three clones. (B, C, E, and F) PhosphorImager scanning of A and D membranes hybridized with (B and F) *EhPgp5*- and (C and E) actin-specific 3'-UTR probes.

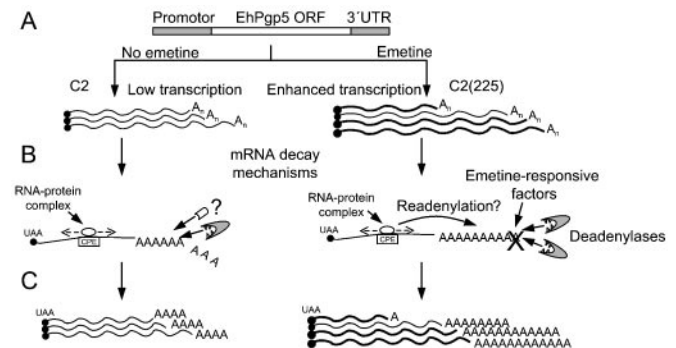


FIG. 8. Working model for *EhPgp5* mRNA expression in C2 cells. A, an enhanced transcription of *EhPgp5* gene occurs in trophozoites of clone C2(225) due to the effect of emetine on the transcriptional factors. ORF, open reading frame. B, in nuclei and cytoplasm, mRNA processing and decay mechanisms influence the *EhPgp5* mRNA half-life. C, trophozoites of clone C2(225) have putative emetine-responsive factors and polyadenylation proteins, which could promote an efficient polymerization of poly(A) tails of certain *EhPgp5* mRNA variants, resulting in a longer poly(A) tail and increased mRNA stability. CPE- and Py-interacting proteins, present in both clones, could promote in clone C2(225)-specific readenylation of *EhPgp5* mRNA due to the expression of emetine-responsive factors, which may also participate in the blockage of the progress of the putative 3'-5' mRNA degradation machinery. Deadenylase activity in trophozoites of clone C2 could be enhanced, resulting in shorter poly(A) tails and diminished *EhPgp5* mRNA half-life. Wave lines denote the *EhPgp5* mRNA, and the filled circle represents the UAA stop codon. Potential Py- and CPE-interacting proteins are indicated as a RNA-protein complex.

DISCUSSION

Previously, we demonstrated that the *EhPgp5* gene is over-expressed in *E. histolytica* trophozoites grown in the presence of high drug concentration (30). Transcriptional factors partic-

ipate in the *EhPgp5* gene promoter activation (11). Results presented here show novel evidence that post-transcriptional *EhPgp5* gene regulation occurs in the drug-resistant trophozoites. *EhPgp5* mRNA is more stable in trophozoites grown in 225 μM emetine than in those grown in 90 μM or without drug (Fig. 2). Additionally, the *EhPgp5* mRNA 3'-UTR length is heterogeneous (Fig. 3A), which may influence the mRNA half-life. The PSIII¹⁵⁶ and PSIV¹⁸⁹ mRNA variants augmented when the emetine dose was increased (Fig. 3, A–E). Their predicted secondary structure suggests that they have exposed a Py tract and a CPE motif (data not shown). Furthermore, a RNA-binding protein complex was detected in their 39-nt shared region (Figs. 5 and 6). In other organisms, polypyrimidine tract-binding proteins have been involved in splicing and stability control of the mRNA, whereas CPE-motif interacting proteins target specific mRNAs to cytoplasmic polyadenylation, producing the translational activation of the transcripts (43–46). Interestingly, the *EhPgp5* mRNA presents a longer poly(A) tail in clone C2(225) (Fig. 7), and it is well known that large poly(A) tails give higher stability to mRNA and promote a more efficient translation (39). Emetine stress could affect the expression of many factors, including the polyadenylation/deadenylation proteins involved in the poly(A) tail length control.

mRNA half-life and translation are linked in ways that are not completely understood. In cells exposed to translation inhibitors some mRNAs are stabilized in several ways, including alterations in polyadenylation rates (22). For example, in mammalian cells, cycloheximide prolongs *c-myc* mRNA half-life by slowing the deadenylation process but does not promote degradation of the mRNA body once deadenylation is being completed (47). The heterogeneity of the *EhPgp5* transcripts is explained by the alternative usage of several polyadenylation signals detected in the 3'-UTR (Fig. 4), as has been well documented for other systems, including other *mdr* genes (40, 48). Mouse *mdr1a* mRNA shows length variations at both 5' and 3' ends, and mRNA variants have very large 3'-UTRs, which are differentially overexpressed in multidrug-resistant cell lines (48). Interestingly, the *EhPgp5* mRNA also presents heterogeneity in the 5' end of trophozoites of clones C2 and C2(225) (11). All these data indicate that *EhPgp5* gene is a complex transcriptional unit whose regulation produces multiple transcript sizes at the 3' and 5' ends.

Emetine partially inhibits protein synthesis in trophozoites of clone C2(225) (data not shown). This could induce a stabilizing mRNA effect (22, 49) affecting certain *EhPgp5* transcript variants. The PSIV¹⁸⁹, PSIII¹⁵⁶, and PSII¹¹⁸ mRNA variants were detected in all clones, whereas PSI¹⁹ was observed only in clone C2(225). PSI¹⁹, PSIII¹⁵⁶, and PSIV¹⁸⁹ transcripts were more abundant in the trophozoites of clone C2(225). PSI¹⁹ transcript, which has a very short poly(A) tail length or is not polyadenylated, was almost 2-fold the amount of PSIII¹⁵⁶ and PSIV¹⁸⁹ in clone C2(225) (Fig. 3). It is possible that the expression of undetermined factors linked to the emetine effect and whose function could be independent of the poly(A) tail contribute to the PSI¹⁹ transcript stability. However, additional experiments are required to confirm this hypothesis.

AURE motifs have been involved in destabilization of mRNAs with a short half-life (42). However, Prokipcak *et al.* (16) find that AUREs at the 3'-UTR of human *MDR1* mRNA is an inefficient promoter of mRNA decay, which suggests that AURE-dependent mRNA stability regulation may not operate in certain cases, such as the *MDR1* and *EhPgp5* mRNAs. This assumption is supported because under the experimental conditions reported here, we did not detect any RNA-protein complex in the AURE motifs present in the *EhPgp5* 3'-UTR mRNA, suggesting that they do not act as *cis*-regulatory elements in

the *EhPgp5* mRNA half-life control.

We found a RNA-protein complex in the proximity of the Py tract in the PSIII¹⁵⁶ and PSIV¹⁸⁹ transcripts (Figs. 5 and 6) that may contribute to their stability in C2(225) cells. However, the same complex was also detected in clones C2 and C2(90), suggesting that other factors present only in clone C2(225) are required to stabilize certain *EhPgp5* mRNA variants. The identity of the 3'-UTR *EhPgp5* mRNA-interacting protein(s) detected here remains to be elucidated. Interestingly, the *EhPgp5* mRNAs from trophozoites of clone C2(225) present longer poly(A) tails than those from C2 and C2(90) cells, suggesting that polyadenylation and deadenylation events, occurring at different rates, could be affecting the *EhPgp5* mRNA half-life.

Our working hypothesis assumes that trophozoites of clone C2 grown without emetine have some factors that maintain short poly(A) tails, which may contribute to a shorter *EhPgp5* mRNA half-life (Fig. 8). Some of these factors could be affected by emetine in C2(225) cells, and emetine-responsive factors could both induce an enhanced polyadenylation of *EhPgp5* mRNAs. The expression and activity of some proteins involved in 3' to 5' exonucleolytic mRNA degradation and polyadenylation may also be participating in the longer *EhPgp5* mRNA half-life in C2(225) cells.² Hence, the putative role of other 3' end processing and polyadenylation/deadenylation factors cannot be discarded.

Acknowledgments—We express gratitude to Drs. Lorena Gutiérrez and Rosa Maria Del Angel for critical reading of this manuscript. Our thanks go also to Alfredo Padilla for help with the artwork.

REFERENCES

- Orozco, E., Pérez, D., Gómez, C., and Ayala, P. (1995) *Parasitol. Today* **11**, 473–475
- Juliano, R. L., and Ling, V. (1976) *Biochim. Biophys. Acta* **455**, 152–162
- Borst, P., and Ouellette, M. (1995) *Annu. Rev. Microbiol.* **49**, 427–460
- Ullman, B. (1995) *J. Bioenerg. Biomembr.* **27**, 77–84
- Endicott, J. A., and Ling, V. (1989) *Annu. Rev. Biochem.* **58**, 137–171
- Johnstone, R. W., Ruefli, A. A., and Smyth, M. J. (2000) *Trends Biochem. Sci.* **25**, 1–6
- Descoteaux, S., Ayala, P., Orozco, E., and Samuelson, J. (1992) *Mol. Biochem. Parasitol.* **54**, 201–211
- Marchat, L., Gómez, C., Pérez, D. G., Paz, F., Mendoza, L., and Orozco, E. (2002) *Cell. Microbiol.* **4**, 725–737
- Orozco, E., López, C., Gómez, C., Pérez, D. G., Marchat, L., Bañuelos, C., and Delgadillo, D. (2002) *Parasitol. Int.* **51**, 353–355
- Gómez, C., Pérez, D. G., López-Bayghen, E., and Orozco, E. (1998) *J. Biol. Chem.* **273**, 7277–7284
- Pérez, D. G., Gómez, C., López-Bayghen, E., Tannich, E., and Orozco, E. (1998) *J. Biol. Chem.* **273**, 7285–7292
- López, C., Gómez, C., Pérez, D. G., Flores, E., and Orozco, E. (1997) *Arch. Med. Res.* **28**, (suppl.) 66–68
- Shen, D. W., Fojo, A., Chin, J. E., Roninson, I. B., Richert, N., Pastan, I., and Gottesman, M. M. (1986) *Science* **232**, 643–645
- Lee, C. H., Bradley, G., and Ling, V. (1995) *Cell Growth Differ.* **6**, 347–354
- Lee, C. H., Bradley, G., and Ling, V. (1998) *J. Cell. Physiol.* **177**, 1–12
- Prokipcak, R. D., Raouf, A., and Lee, C. (1999) *Biochem. Biophys. Res. Commun.* **261**, 627–634
- Lee, C. H. (2001) *Mol. Cell. Biochem.* **216**, 103–110
- McClellan, S., and Hill, B. T. (1993) *Eur. J. Cancer* **29**, 2243–2248
- Muller, C., Laurent, G., and Ling, V. (1995) *J. Cell. Physiol.* **163**, 538–544
- Zhang, W., and Ling, V. (2000) *J. Cell. Physiol.* **184**, 17–26
- Shaw, G., and Kamen, R. (1986) *Cell* **46**, 659–667
- Ross, J. (1995) *Microbiol. Rev.* **59**, 423–450
- Ross, J. (1996) *Trends Genet.* **12**, 171–175
- Decker, C. J., and Parker, R. (1995) *Curr. Opin. Cell Biol.* **7**, 386–392
- Zhao, J., Hyman, L., and Moore, C. (1999) *Microbiol. Mol. Biol. Rev.* **63**, 405–445
- Sachs, A. (2000) in *Translational Control of Gene Expression* (Sonenberg, N., Hershey, J. W. B., and Mathews, M. B., eds) pp. 447–465, Cold Spring Harbor Laboratory Press, Cold Spring Harbor, NY
- Wilusz, C. J., Wormington, M., and Peltz, S. W. (2001) *Nat. Rev. Mol. Cell Biol.* **2**, 237–246
- Orozco, E., Hernandez, F., and Rodriguez, M. (1985) *Mol. Biochem. Parasitol.* **15**, 49–59
- Diamond, L. S., Harlow, R., and Cunnick, C. (1978) *Trans. R. Soc. Trop. Med. Hyg.* **72**, 431–432
- Descoteaux, S., Ayala, P., Samuelson, J., and Orozco, E. (1995) *Gene (Amst.)* **164**, 179–184

² C. López-Camarillo, J. P. Luna-Arias, L. A. Marchat, and E. Orozco, unpublished results.

31. Edman, U., Meza, I., and Agabian, N. (1987) *Proc. Natl. Acad. Sci. U. S. A.* **4**, 3024–3028
32. Belasco, J. G., and Brawerman, G. (1993) in *Control of Messenger RNA Stability* (Belasco, J. G., and Brawerman, G., eds) pp. 475–493, Academic Press, San Diego, CA
33. Schreiber, E. (1989) *Nucleic Acids Res.* **17**, 6419
34. Bradford, M. (1976) *Anal. Biochem.* **72**, 248–254
35. Sallés, F. J., and Strickland, S. (1995) *PCR Methods Applications.* **4**, 317–321
36. Delgadillo, D. M., Perez, D. G., Gomez, C., Ponce, A., Paz, F., Bañuelos, C., Mendoza, L., Lopez, C., and Orozco, E. (2002) *Microb. Drug Resist.* **8**, 15–26
37. Chrzanowska-Lightowlers, Z., Preiss, T., and Lightowlers, R. (1994) *J. Biol. Chem.* **269**, 27322–27328
38. Higgins, C. F., Causton, H. C., Dance, G. S. G., and Mudd, E. A. (1993) in *Control of Messenger RNA Stability* (Belasco, J. G., and Brawerman, G., eds) pp. 13–30. Academic Press, San Diego, CA
39. Wickens, M., Anderson, P., and Jackson, R. J. (1997) *Curr. Opin. Genet. Dev.* **7**, 220–232
40. Edwalds-Gilbert, G., Veraldi, K. L., and Milcarek, C. (1997) *Nucleic Acids Res.* **25**, 2547–2561
41. Bruchhaus, I., Leippe, M., Lioutas, C., and Tannich, E. (1993) *DNA Cell Biol.* **12**, 925–933
42. Chen, C. Y., and Shyu, A. B. (1995) *Trends Biochem. Sci.* **20**, 465–470
43. Hake, L., Mendez, R., and Ritcher, J. D. (1998) *Mol. Cell. Biol.* **63**, 685–693
44. Tillmar, L., Carlsson, C., and Welsh, N. (2002) *J. Biol. Chem.* **277**, 1099–1106
45. Irwin, N., Baekelandt, V., Goritchenko, L., and Benowitz, L. I. (1997) *Nucleic Acids Res.* **25**, 1281–1288
46. Czyzyk-Krzeska, M. F., Dominski, Z., Kole, R., and Millhorn, D. E. (1994) *J. Biol. Chem.* **269**, 9940–9945
47. Laird-Offringa, L., De Wit, C., Elfferich, P., and Van Der Eb, A. (1990) *Mol. Cell. Biol.* **10**, 6132–6140
48. Hsu, S. I., Cohen, D., Kirschner, L. S., Lothstein, L., Hartstein, M., and Horwitz, S. B. (1990) *Mol. Cell. Biol.* **10**, 3596–3606
49. Entner, N., and Grollman, A. P. (1973) *J. Protozool.* **20**, 160–163

**EhPgp5 mRNA Stability Is a Regulatory Event in the *Entamoeba histolytica*
Multidrug Resistance Phenotype**

César López-Camarillo, Juan Pedro Luna-Arias, Laurence A. Marchat and Esther Orozco

J. Biol. Chem. 2003, 278:11273-11280.

doi: 10.1074/jbc.M211757200 originally published online January 28, 2003

Access the most updated version of this article at doi: [10.1074/jbc.M211757200](https://doi.org/10.1074/jbc.M211757200)

Alerts:

- [When this article is cited](#)
- [When a correction for this article is posted](#)

[Click here](#) to choose from all of JBC's e-mail alerts

This article cites 46 references, 11 of which can be accessed free at
<http://www.jbc.org/content/278/13/11273.full.html#ref-list-1>